ISSUE: August 2019

The Engineer's Guide To EMI In DC-DC Converters (Part 9): Spread-Spectrum Modulation

by Timothy Hegarty, Texas Instruments, Phoenix, Ariz.

The reduction of electromagnetic interference (EMI) is an inherent problem in all electronic systems, as evidenced by the many specifications that link electromagnetic compatibility (EMC) with the ability to fit the interfering power spectrum level under a prescribed mask.[1] For high-frequency switching dc-dc converters in particular, the presence of high slew-rate voltages and currents during switching commutations may generate severe conducted and radiated interference within the regulator itself (the EMI source) as well as nearby susceptible circuits (the EMI victims). Parts 5 and 6 of this article series[1-8] reviewed several EMI mitigation techniques for nonisolated regulator designs. Parts 7 and 8 reviewed common-mode (CM) noise and its abatement in isolated designs.

In general, complying with electromagnetic standards is an increasingly important task for switching power supplies. This is not because the power supplies are sources of excessive total spectral energy, but more so that they generate concentrated energy in specific narrow bands at the fundamental switching frequency and its harmonics. To that end, this part 9 discusses spread-spectrum frequency modulation (SSFM) as a way to distribute spectral energy in the frequency domain and thus flatten the fundamental and harmonic noise peak amplitudes. The spread-spectrum effect shown in Fig. 1 is available as an additional and complementary method of noise reduction with respect to the EMI mitigation techniques described in previous installments of this article series.

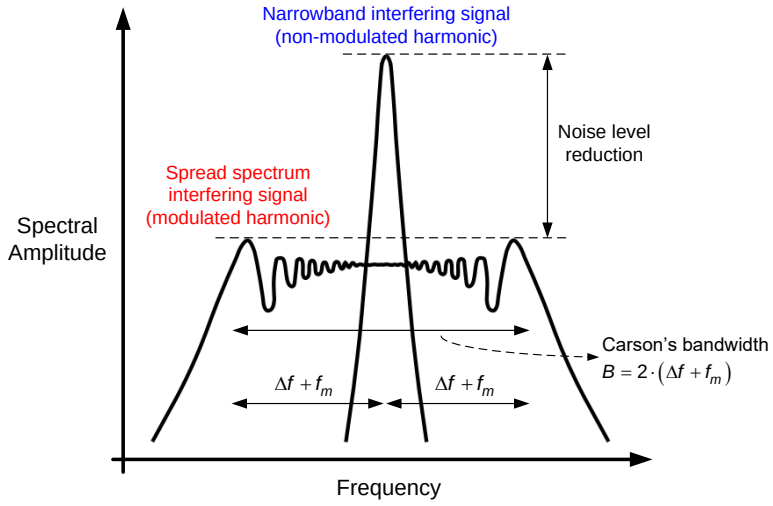

Fig. 1. Spread-spectrum effect.

Spread-Spectrum Modulation

The EMI mitigation techniques discussed in parts 5 and 6 of this article series focused on reducing the antenna factor through careful layout of high slew-rate current (di/dt) loops and avoiding sharp transient voltages (dv/dt) through suitable snubber and gate-drive circuit design. Effective mostly at high frequencies, these methods seek to adjust the shape of the conducted and/or radiated noise power spectrum by reducing its overall power. The effectiveness at low frequencies may be limited, though.

Conversely, spread-spectrum modulation (or dithering), first proposed in 1992 for dc-dc converters,[9] aims to reshape the conducted and radiated interfering power spectrum without affecting the total noise power. Through frequency modulation (FM) of the reference clock signal in the time domain, the fundamental and harmonic components are swept in the frequency domain according to the modulating signal.[9-14] As depicted in Fig. 1, each harmonic changes into a number of sideband harmonics with lower amplitudes. The noise spectrum

alters from a train of large spectral peaks concentrated at the switching frequency and its harmonics to a smoother, lower and more continuous spectrum.

From a practical EMC standpoint, when a narrowband EMI source's signal frequency aligns with an EMI victim's sensitive frequency range, a large amount of power can transfer in a given time window, increasing the probability of disturbance or failure of the EMI victim. Spreading the EMI source signal into a bandwidth larger than the EMI victim's sensitivity bandwidth reduces the noise power coupled to the victim, leading to an overall improvement in EMC performance and reliability.

Periodic Modulation Functions

The main idea behind periodic spread-spectrum modulation techniques is to spread each individual harmonic into a preset frequency band, leading to reduced peak amplitudes and lower EMI levels. Within this context, equation 1 provides a generalized analytical expression for frequency modulation of a sinusoidal carrier due to spread-spectrum modulation:

$$s(t) = A \cdot \cos\left(2\pi f_c t + 2\pi \Delta f \int_{-\infty}^{t} \xi(t) d\tau\right) \qquad (1)$$

where A is the amplitude of the unmodulated signal, f_c is the carrier frequency and Δf is the frequency deviation.

The normalized periodic modulating function is $\xi(t)$, which expresses the frequency variation of the spread spectrum. Table 1 gives the mathematical expressions for sinusoidal, triangular and exponential (also known as cubic or "Hershey's Kiss") modulation profiles.[10] Here, k_T is a symmetry index of the triangular profile that ranges from 0 to 1, and p designates a concavity coefficient of the exponential profile. The triangular profile has a symmetrical triangular pattern if k_T is 0.5.

Table 1. Sinusoidal, triangular and exponential modulation profiles where f_m and T_m are the modulating signal frequency and period, respectively.

Sinusoidal	Triangular (with symmetry index, k_T)	Exponential (with concavity coefficient, p)
$\xi(t) = \sin(2\pi f_m t)$	$\xi(t) = \begin{cases} \frac{2}{k_T} \cdot f_m t, & 0 \le t < \frac{k_T \cdot T_m}{2} \\ \frac{1}{1-k_T} \cdot (1 - 2 f_m t), & \frac{k_T \cdot T_m}{2} \le t < \left(1 - \frac{k_T}{2}\right) \cdot T_m \\ \frac{2}{k_T} \cdot (f_m t - 1), & \left(1 - \frac{k_T}{2}\right) \cdot T_m \le t < T_m \end{cases}$	$\xi(t) = \begin{cases} \frac{1}{e^{p/4 \cdot f_m} - 1} \cdot \left(e^{p \cdot t} - 1\right), & 0 \le t < \frac{T_m}{4} \\ \frac{1}{e^{p/4 \cdot f_m} - 1} \cdot \left(e^{p/2 \cdot f_m} \cdot e^{-p \cdot t} - 1\right), & \frac{T_m}{4} \le t < \frac{T_m}{2} \\ \frac{1}{e^{p/4 \cdot f_m} - 1} \cdot \left(1 - e^{-p/2 \cdot f_m} \cdot e^{p \cdot t}\right), & \frac{T_m}{2} \le t < \frac{3 \cdot T_m}{4} \\ \frac{1}{e^{p/4 \cdot f_m} - 1} \cdot \left(1 - e^{p/f_m} \cdot e^{-p \cdot t}\right), & \frac{3 \cdot T_m}{4} \le t < T_m \end{cases}$

Fig. 2 shows the sinusoidal, triangular and exponential modulating signals with a 10-kHz modulating frequency. Also captured is the corresponding spread-spectrum result by modulating a 100-kHz sinusoidal carrier signal consistent with equation 1. The top of each plot specifies notable instantaneous carrier working frequencies.

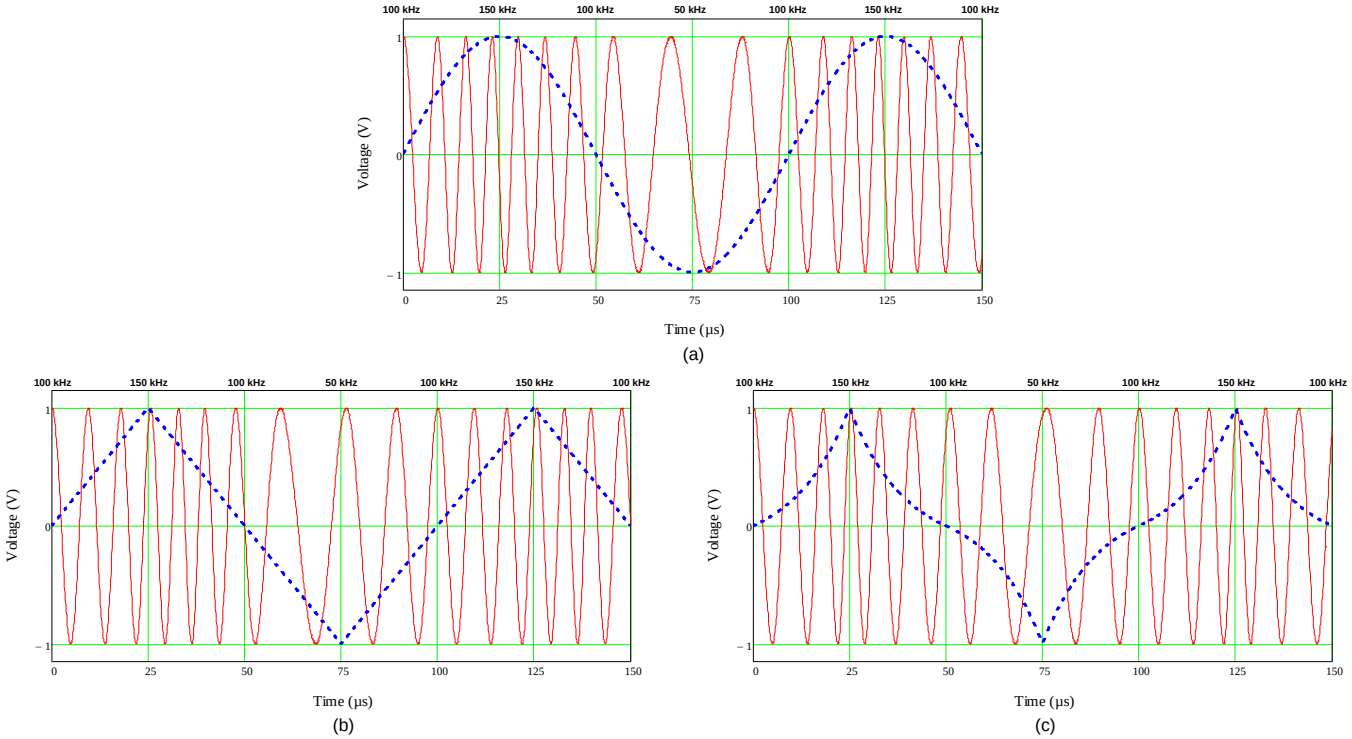

Fig. 2. Sinusoidal (a), triangular (b) and exponential (c) modulation profiles with f_c = 100 kHz, Δf = 50 kHz, f_m = 10 kHz, k_T = 0.5 and p = 70 kHz.

Other relevant terms are the modulation index and modulation ratio given by equations 2 and 3, respectively:

$$m = \frac{\Delta f}{f_m} = \Delta f \cdot T_m \qquad (2)$$

$$\delta = \frac{\Delta f}{f_c} \qquad (3)$$

The total power of *s(t)* is equal to $A^2/2$, which is distributed using the spread-spectrum technique according to Carson's bandwidth rule—that is, the energy after spread spectrum is 98% contained in a bandwidth, B (see Fig. 1), given by Equation 4:

$$\mathrm{B} = 2 \cdot \left(\Delta f + f_m\right) = 2 \cdot f_m \cdot \left(1 + m\right) \qquad (4)$$

For a more complicated waveform, such as the switch-node voltage or the input current of a dc-dc converter, changing the instantaneous frequency is equivalent to applying equation 1 to each constituent harmonic of the Fourier series expansion, with the only difference being that the *n*th harmonic is spread within a bandwidth of *n* times Carson's bandwidth given by equation 5.

$$\rho = \frac{\mathrm{RBW}\,(-3dB)}{\Delta f} = \frac{6\,\mathrm{kHz}}{105\,\mathrm{kHz}} = 0.057 \qquad (5)$$

The actual shape of the spectrum of $s(t)$ depends on the modulation parameters Δf and $\xi(t)$. When $\xi(t)$ is a periodic function with period T_m, the spectrum of $s(t)$ is discrete, meaning that it is possible to decompose the signal into a sum of sinusoidal tones at frequency $f_c \pm k/T_m$, each one with amplitude A_k. The computation of A_k

for sinusoidal modulation is achieved with Bessel functions,[9, 10] while the spectrum shape for triangular modulation has been evaluated using a Matlab simulation.[11]

A truly continuous power spectrum in the frequency domain is obtained only with a nonperiodic modulating function such as that achieved using a chaotic or random sequence generator, and is described using the power spectral density. A nonperiodic modulation, in contrast to a periodic spreading technique, allows a measured spectral shape independent of the resolution bandwidth (RBW) setting[15, 16] of the measurement instrument. I will examine the impact of RBW on the EMI measurement in the next section.

While a sinusoidal spreading technique is easier to analyze and implement, it does not yield the best spectrum shape, and the harmonic attenuation is not maximized. As illustrated in Fig. 3, the energy in the spectrum of the modulated waveform tends to concentrate at frequencies corresponding to points in the modulation waveform where the time derivative is low, which is near the peaks and valleys of a sinusoidal waveform.

On the other hand, the exponential modulating function has the flattest spectrum and further reduces EMI by compensating for the peaks due to second-order effects that appear near both ends of Carson's bandwidth. However, the exponential waveform is difficult to implement in practice, typically requiring a complex distortion circuit or a look-up table.

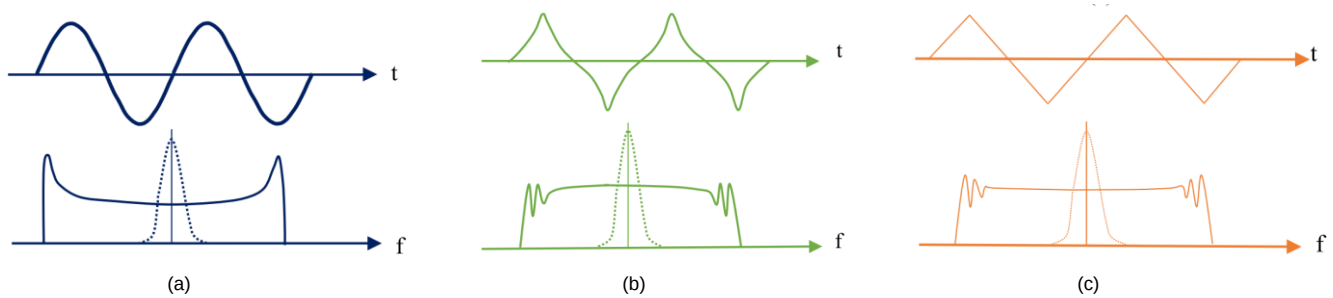

Fig. 3. Sinusoidal (a), triangular (b) and exponential (c) periodic modulation functions and frequency-domain behaviors.

A linear, triangular-shaped modulation represents a good compromise between the modulation profiles illustrated in Fig. 3 and is easy to implement in both the analog and digital domains. By selecting an optimized, well-defined frequency of the triangular driving signal to achieve maximum peak reduction of the measured EMI spectrum, you can realize a robust design for high-volume and cost-optimized applications such as automotive.

EMI Reduction Optimization By Spread Spectrum

International regulations require measurements to be taken with an EMI receiver, essentially an analog spectrum analyzer with some additional input filters. Given the complexity of the superheterodyne spectrum analyzer[16] (in particular, the nonlinearity of the demodulating envelope detector and the peak/quasi-peak/average detector) for EMI measurements, researchers in reference [11] used a Matlab model of an EMI receiver to calculate reduced EMI via spreading techniques based on a triangular modulation. This enabled the development of optimization curves for triangular spread spectrum.

As an example, Fig. 4 provides curves for noise-level reduction based on several values of frequency deviation Δf as a multiple of the RBW setting of the EMI receiver. Notice that the EMI reduction performance reduces when m increases above a certain value.

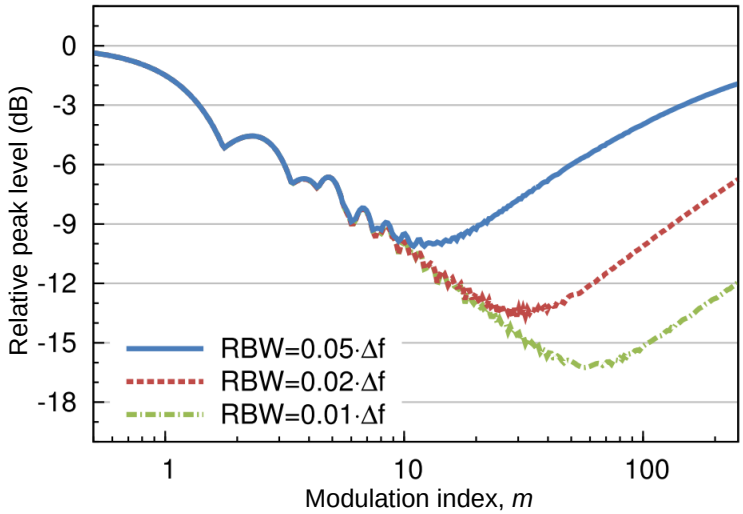

Fig. 4. Noise-level reduction of the triangular modulation power spectrum consistent with the EMI receiver response for different ratios of RBW/Δf, where the modulation index is varied by fixing Δf and changing f_m. The 0-dB reference is the unmodulated case.

Two tradeoffs exist when selecting modulation spreading parameters Δf and f_m. First, Δf should be large enough to reduce the measured EMI as well as the interference of the EMI victim. For example, in order to avoid interference within the AM radio band, an automotive dc-dc regulator typically uses an external resistor to set the free-running switching frequency at 2.1 MHz with a 5% to 10% allowable tolerance. To operate above the maximum AM band frequency of 1.6 MHz with adequate margin, a center-spread modulation with Δf in the range of 100 kHz to 150 kHz is appropriate, and avoids large perturbations to the regulator's output voltage ripple amplitude and efficiency performance.

Having established Δf, an additional degree of freedom to optimize EMI performance depends on the choice of modulating frequency. The modulation index m should have an intermediate value according to Fig. 4. That is, m should be high enough to provide EMI attenuation yet low enough that the time-domain effect of the RBW bandpass filter is not applicable.

More specifically, if f_m is low, the time interval in which the instantaneous interfering signal frequency is within the RBW filter response time increases. The signal appears unmodulated for a longer time in the measurement window, effectively resulting in a measurement of the unmodulated signal amplitude. This short-term time domain effect similarly applies to an EMI victim circuit and its sensitivity band.

As a result, a consideration of the time-domain behavior is essential for a correct estimation of the impact of spreading techniques when using the appointed EMI measurement setup over the prescribed frequency range. For example, regulations such as CISPR 25 for automotive applications impose RBW settings of 9 kHz and 120 kHz for measurements in the frequency bands of 150 kHz to 30 MHz and 30 MHz to 1 GHz, respectively. As a general rule of thumb, when setting f_m close to the mandated RBW, the EMI receiver is able to measure each individual sideband harmonic separately such that the measurement results tally with the expected calculations.

Practical Case Study

Fig. 5 shows the schematic of a four-phase synchronous buck regulator circuit[17] using two dual-phase stackable controllers. The controller incorporates several features for EMI reduction, including constant switching-frequency operation, external clock synchronization and switch-node shaping (slew-rate control) with split gate-drive outputs for each power switch.

The controller operates with a resistor-adjustable switching frequency up to 2.2 MHz, with external synchronization possible up to 2.5 MHz. Three options are available to configure the SSFM:

- Apply a carrier frequency signal with the required modulation using the controller's external synchronization (SYNCIN) input.
- Resistively couple a modulation signal to the RT pin.[18]
- Set the modulating frequency with a capacitor at the DITH pin and use the built-in ±5% triangular spread-spectrum (dither) function.

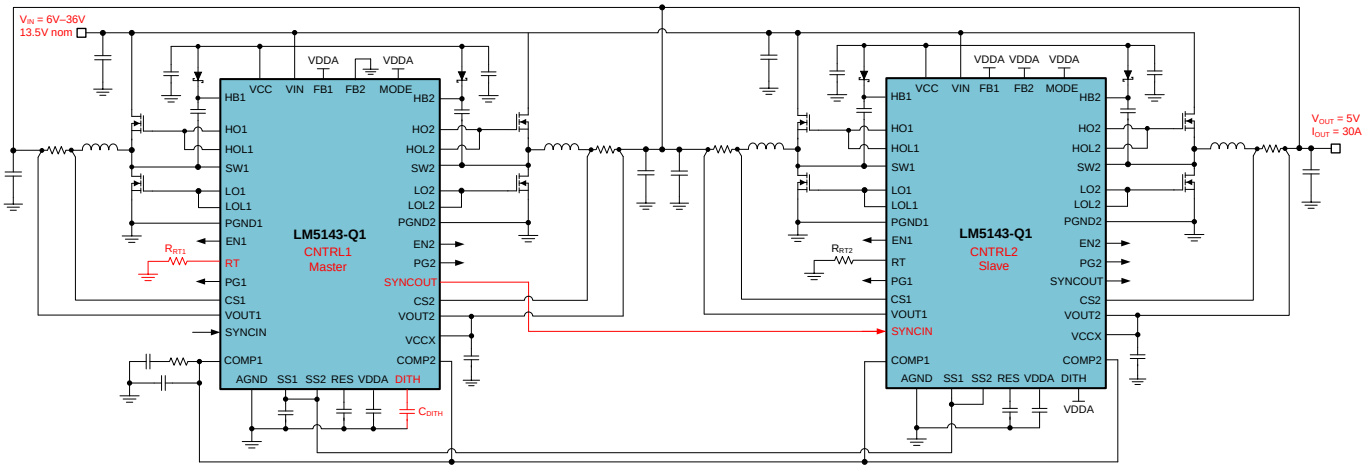

Fig. 5. Schematic of a four-phase synchronous buck regulator with triangular spread-spectrum modulation.

Given a nominal switching frequency of 2.1 MHz, the frequency deviation Δ*f* is 5% or 105 kHz when using the integrated spread-spectrum feature. The EMI receiver uses an RBW filter of 9 kHz for measurements in the range of 150 kHz to 30 MHz. Since EMI filters in spectrum analyzers are usually defined in terms of a -6-dB bandwidth with a four-pole, nearly Gaussian shape,[16] applying a correction factor finds the effective -3-dB bandwidth of the 9-kHz RBW filter as approximately 6 kHz. Using equation 5 (repeated below) to calculate the normalized resolution finds an optimized modulation index of approximately 10 based on optimization curves similar to Fig. 4:

$$\rho = \frac{\mathrm{RBW}(-3dB)}{\Delta f} = \frac{6\,\mathrm{kHz}}{105\,\mathrm{kHz}} = 0.057$$

The required modulating frequency is then derived using Equation 6:

$$f_m = \frac{\Delta f}{m} = \frac{105\,\mathrm{kHz}}{10} = 10.5\,\mathrm{kHz} \qquad (6)$$

Fig. 6 shows the switch-node voltage waveform (measured using the regulator in Fig. 5) with spread spectrum both enabled and disabled. The waveform of Fig. 6b has scope persistence activated to illustrate the switching frequency variation.

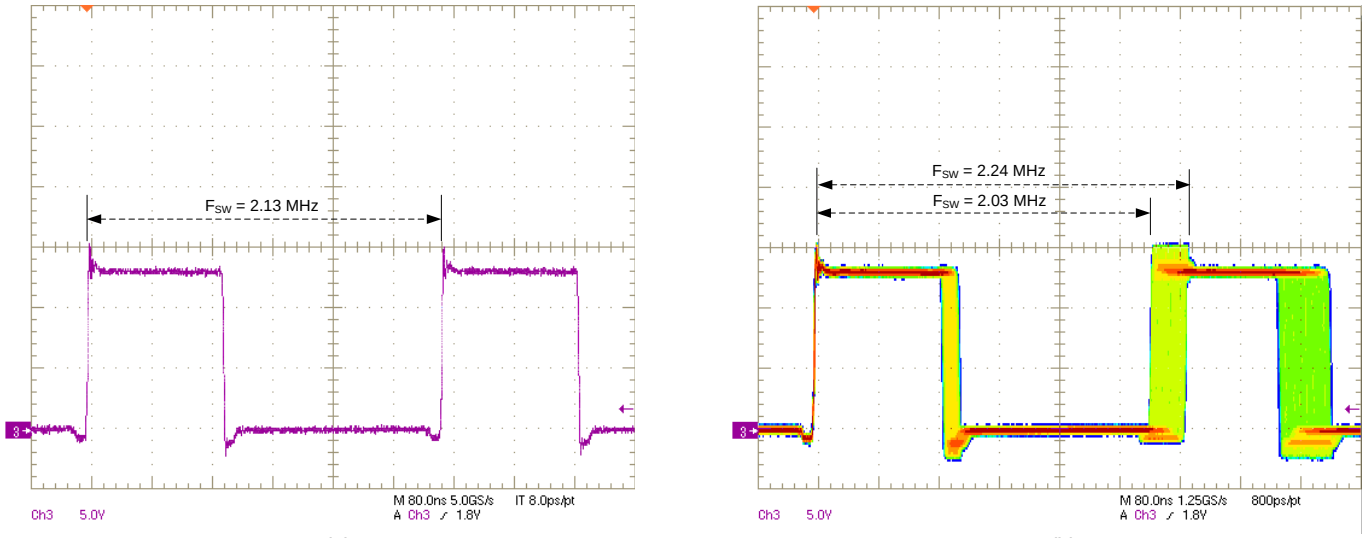

(a) (b)

Fig. 6. Switch-node voltage waveform (V_{IN} = 13.5 V, V_{OUT} = 5 V and I_{OUT} = 20 A) with spread spectrum disabled (a) and enabled (b).

Fig. 7 shows the conducted emissions measured from 150 kHz to 30 MHz for the regulator in Fig. 5 with a triangular modulation function set at 10 kHz. Using a Rohde & Schwarz spectrum analyzer, peak and average detector scans are denoted in yellow and blue, respectively. The results are in compliance with CISPR 25 Class 5 requirements. The limit lines in red are the Class 5 peak and average limits (peak limits are generally 20 dB higher than the average limits).

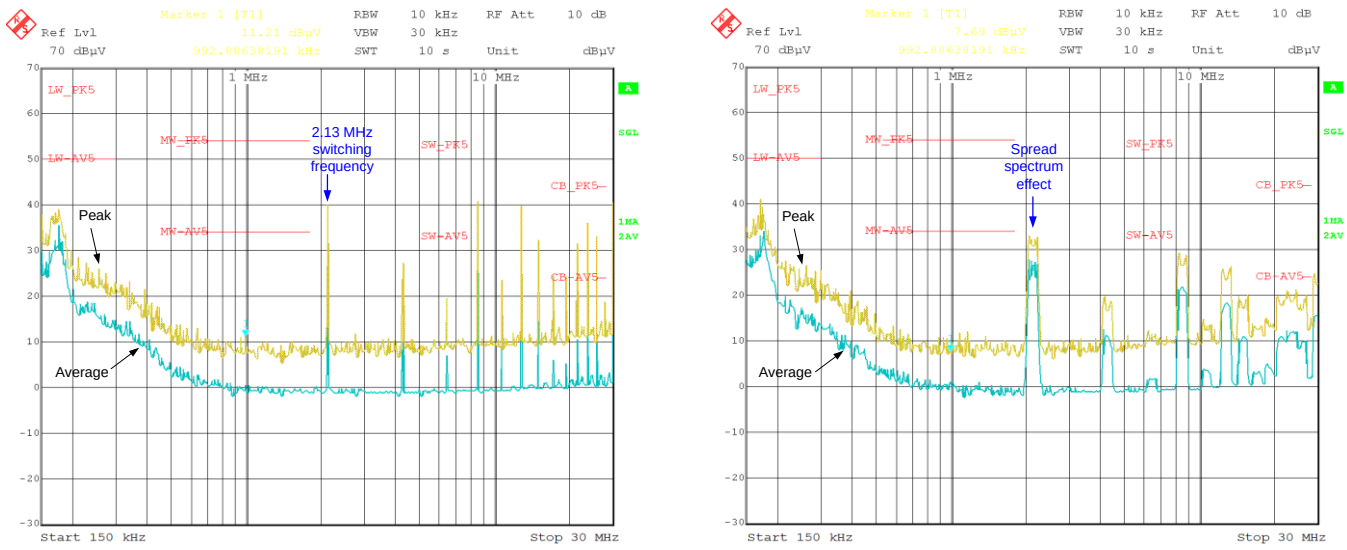

(a) (b)

Fig. 7. CISPR 25 Class 5 conducted emission results (150 kHz to 30 MHz) with spread spectrum disabled (a) and enabled (b).

Summary

With a crowded electromagnetic spectrum, switching power supplies are a key contributor to the deterioration of the electromagnetic environment. Spread-spectrum techniques seek to alter the shape of the conducted and radiated interfering power spectrum, reducing the level of peak emissions as required by international EMC

regulations. The selection of an optimized modulating frequency results in a system-level solution with a smaller footprint and volume, a lower intrinsic cost, and a higher power density.

References

1. "The Engineer's Guide To EMI In DC-DC Converters (Part 1): Standards Requirements And Measurement Techniques" by Timothy Hegarty, How2Power Today, December 2017 issue.
2. "The Engineer's Guide To EMI In DC-DC Converters (Part 2): Noise Propagation and Filtering" by Timothy Hegarty, How2Power Today, January 2018 issue.
3. "The Engineer's Guide To EMI In DC-DC Converters (Part 3): Understanding Power Stage Parasitics" by Timothy Hegarty, How2Power Today, March 2018 issue.
4. "The Engineer's Guide To EMI In DC-DC Converters (Part 4): Radiated Emissions" by Timothy Hegarty, How2Power Today, April 2018 issue.
5. "The Engineer's Guide To EMI In DC-DC Converters (Part 5): Mitigation Techniques Using Integrated FET Designs" by Timothy Hegarty, How2Power Today, June 2018 issue.
6. "The Engineer's Guide To EMI In DC-DC Converters (Part 6): Mitigation Techniques Using Discrete FET Designs" by Timothy Hegarty, How2Power Today, September 2018 issue.
7. "The Engineer's Guide To EMI In DC-DC Converters (Part 7): Common-Mode Noise Of A Flyback" by Timothy Hegarty, How2Power Today, December 2018 issue.
8. "The Engineer's Guide To EMI In DC-DC Converters (Part 8): Mitigation Techniques For Isolated Designs," by Timothy Hegarty, How2Power Today, February 2019 issue.
9. "Reduction of power supply EMI emissions by switching frequency modulation," by Feng Lin, master's thesis, Virginia Tech, August 1992.
10. "EMI reduction in switched power converters using frequency modulation techniques," by Josef Balcells et al., *IEEE Transactions on Electromagnetic Compatibility* 47, No. 3 (August 2005): pp. 569-576.
11. "EMI reduction via spread spectrum in DC/DC converters: state of the art, optimization, and tradeoffs," by Fabio Pareschi et al., *IEEE Access* 3 (December 2015): pp. 2857-2874.
12. "Practical optimization of EMI reduction in spread spectrum clock generators with application to switching DC/DC converters," by Fabio Pareschi et al., *IEEE Transactions on Power Electronics* 29, No. 9 (September 2014): pp. 4646-4657.
13. "Understanding noise-spreading techniques and their effects in switch-mode power applications," white paper and presentation, by John Rice et al., Texas Instruments Power Supply Design Seminar SEM1800, 2008-2009.
14. "A review of spread-spectrum-based PWM techniques – A novel fast digital implementation," by Rabiaa Gamoudi et al., *IEEE Transactions on Power Electronics* 33, No. 12 (December 2018): pp. 10292-10307.
15. "Making EMI compliance measurements," application note, Keysight Technologies, 2015.
16. "Spectrum analysis basics," application note 150, Keysight Technologies, 2016.
17. "LM5143-Q1 four-phase synchronous buck regulator design for automotive ADAS applications," by Timothy Hegarty, Texas Instruments application report, March 2019.
18. "Frequency Dithering: A Tool for Overcoming Last-Minute EMC Hurdles," by Bob Bell and Ajay Hari, How2Power Today, September 2009 issue.

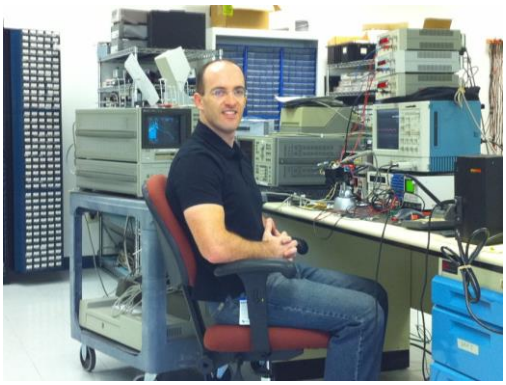

About The Author

Timothy Hegarty is an applications engineer for the Buck Switching Regulators business unit at Texas Instruments. With over 20 years of power management engineering experience, he has written numerous conference papers, articles, seminars, white papers, application notes and blogs.

Tim's current focus is on enabling technologies for high-frequency, low-EMI, isolated and nonisolated regulators with wide input voltage range, targeting industrial, communications and automotive applications in particular. He is a senior member of the IEEE and a member of the IEEE Power Electronics, Industrial Applications and EMC Societies.

For more information on EMI, see How2Power's Power Supply EMI Anthology. Also see the How2Power's Design Guide, locate the Design Area category and select "EMI and EMC".